Application of Cryo-copper Accelerating Structures Towards Future Light Sources

Emilio Nanni
FLS 2023
8/29/2023

Acknowledgements

Submitted to the Proceedings of the US Community Study
on the Future of Particle Physics (Snowmass 2021)

SLAC-PUB-17661
April 12, 2022

Strategy for Understanding the Higgs Physics:
The Cool Copper Collider

SLAC-PUB-17660
April 12, 2022

C^3 Demonstration Research and Development Plan

SLAC-PUB-17629
November 1, 2021

C^3 : A "Cool" Route to the Higgs Boson and Beyond

arXiv > hep-ex > arXiv:2307.04084

High Energy Physics – Experiment

[Submitted on 9 Jul 2023]

A Sustainability Roadmap for C^3

Community Events

Fermilab, SLAC, LANL &
Snowmass Session in Seattle

Cornell Aug. 31st-Sept. 1st

https://indico.classe.cornell.edu/event/2283/overview

https://sites.google.com/view/ec4c3

More Details Here (Follow, Endorse, Collaborate):
https://web.slac.stanford.edu/c3/

Particle Accelerators Drive Scientific Discovery

Coherent X-rays from LCLS (2009)

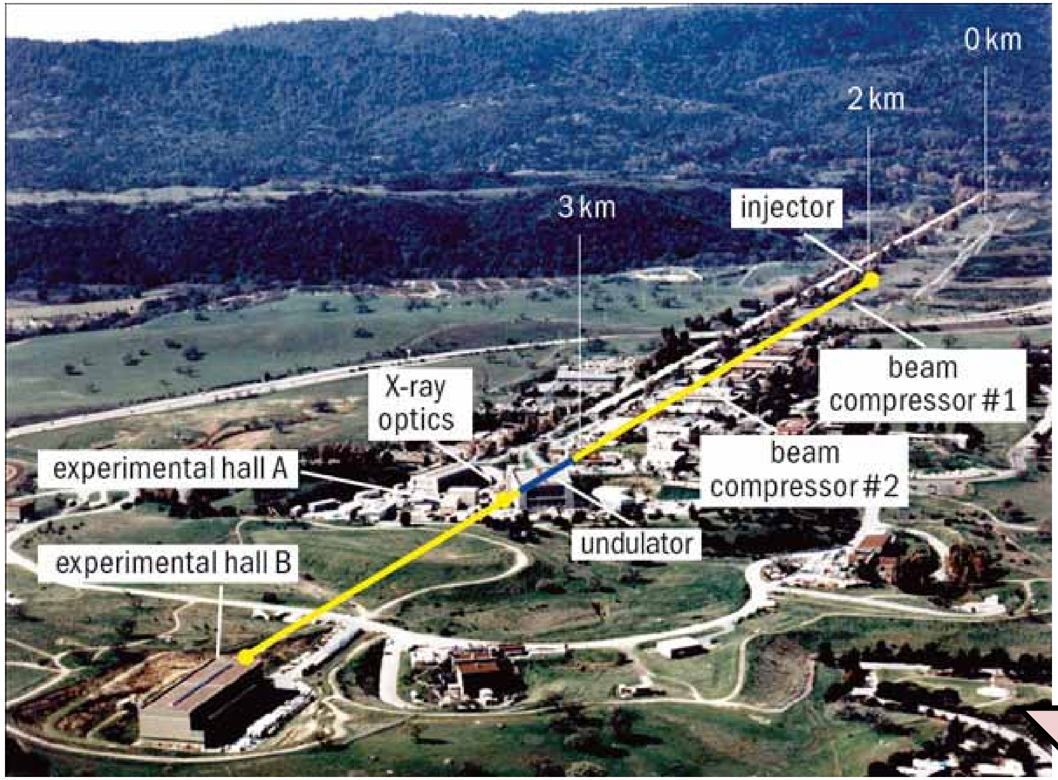

Ultrafast Electron Diffraction (2015)

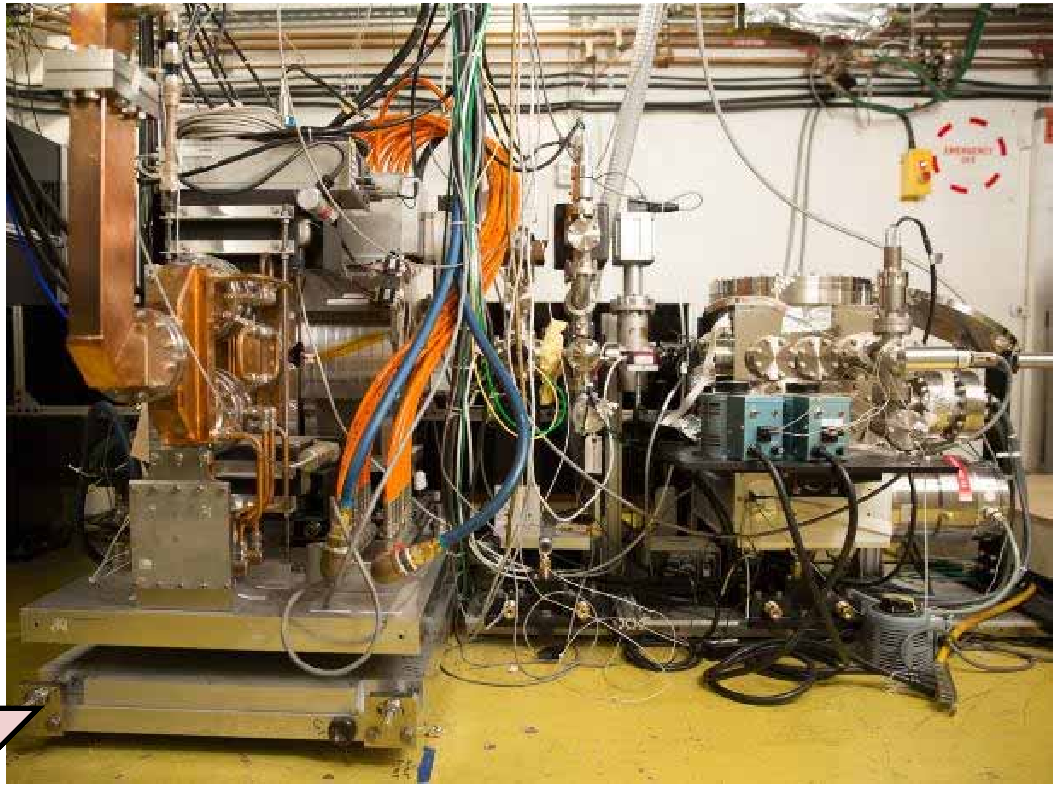

How do we improve gradient, stability, repetition rate and brightness?

What Sets the Limit on Accelerating Gradient?

- Breakdowns depend strongly on electric field strength in structure
- Between structures limits are closely tied to peak magnetic field(!)
- High gradients induce stress (pulsed heating) in material surface leading to damage
- Mitigate by using harder alloys of copper - CuAg

Single Cell C-band Structure

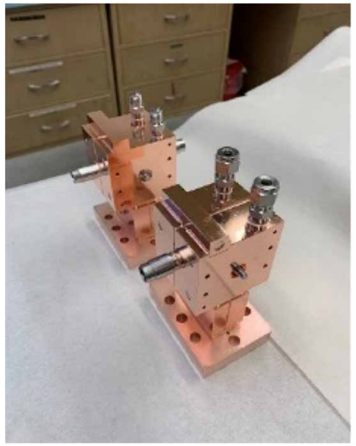

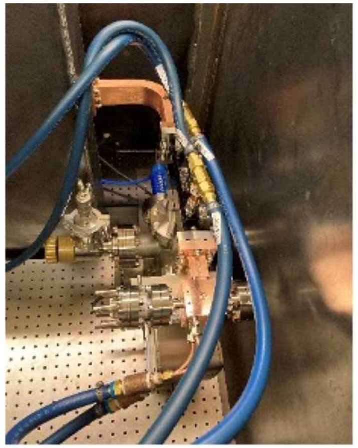

Peak Electric Field

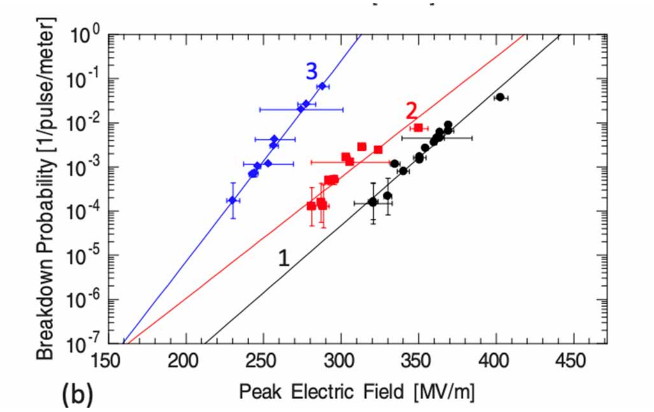

Peak Magnetic Field

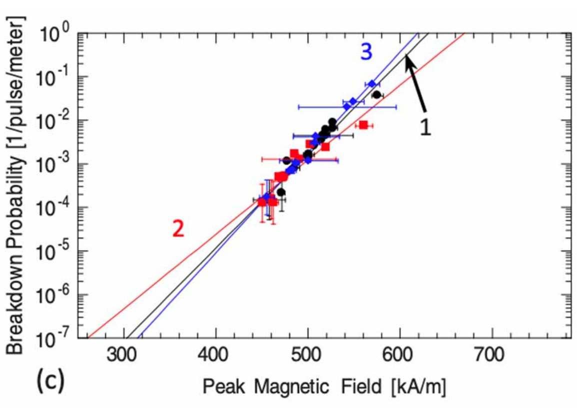

APPLIED PHYSICS LETTERS 97, 171501 2010

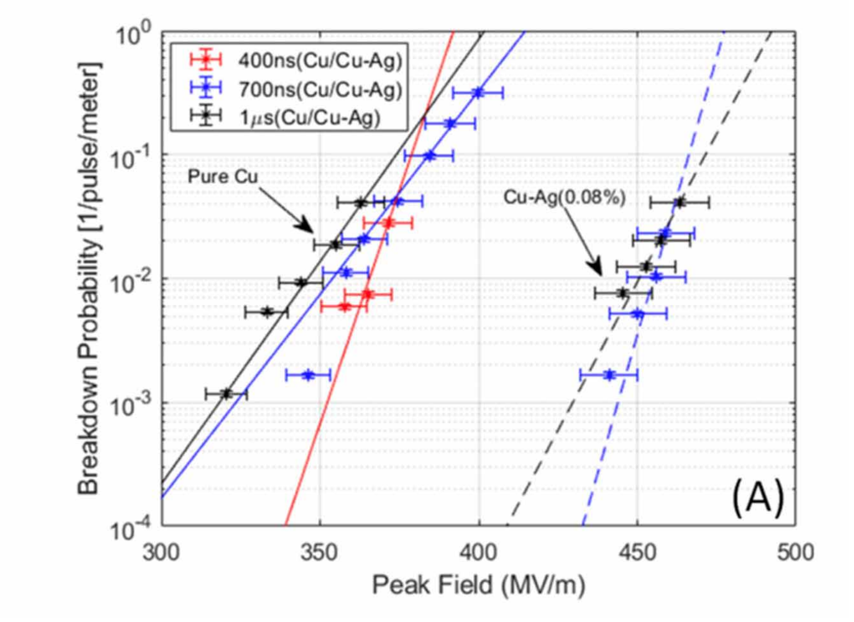

Applied Physics Letters 121.25 (2022).

Reducing Pulsed Heating with Cryogenic Operation

- Increased material conductivity at cryogenic temperature
- Significant reduction in pulsed heating
- Yield strength and thermal diffusion both increase

Surface Resistance

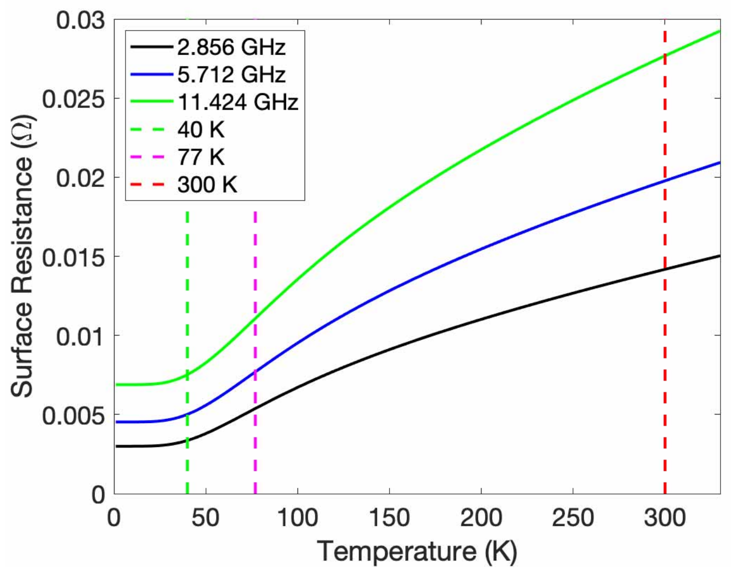

Pulsed Heating

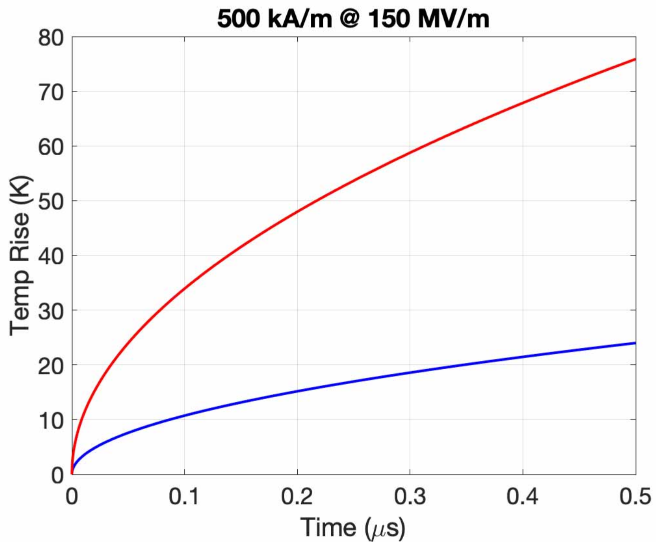

C-band Re-Entrant Cell

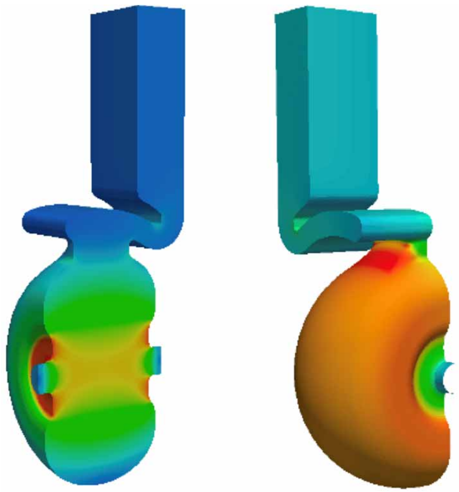

- **Additional Benefits: ~3X reduction in rf sources, ~3X reduction in rf losses, ~3X increase in Q**

Journal of Instrumentation 18.07 (2023): P07053.

Cryo-Copper: Enabling Efficient High-Gradient Operation

Cryogenic temperature elevates performance in gradient

- Increased material strength is key factor
- Increase electrical conductivity reduces pulsed heating in the material

Operation at 77 K with liquid nitrogen is simple and practical

- Large-scale production, large heat capacity, simple handling
- Small impact on electrical efficiency

$$\eta_{cp} = LN\ Cryoplant$$
$$\eta_{cs} = Cryogenic\ Structure$$
$$\eta_k = RF\ Source$$

$$\frac{\eta_{cs}}{\eta_k}\eta_{cp} \approx \frac{2.5}{0.5}[0.15] \approx 0.75$$

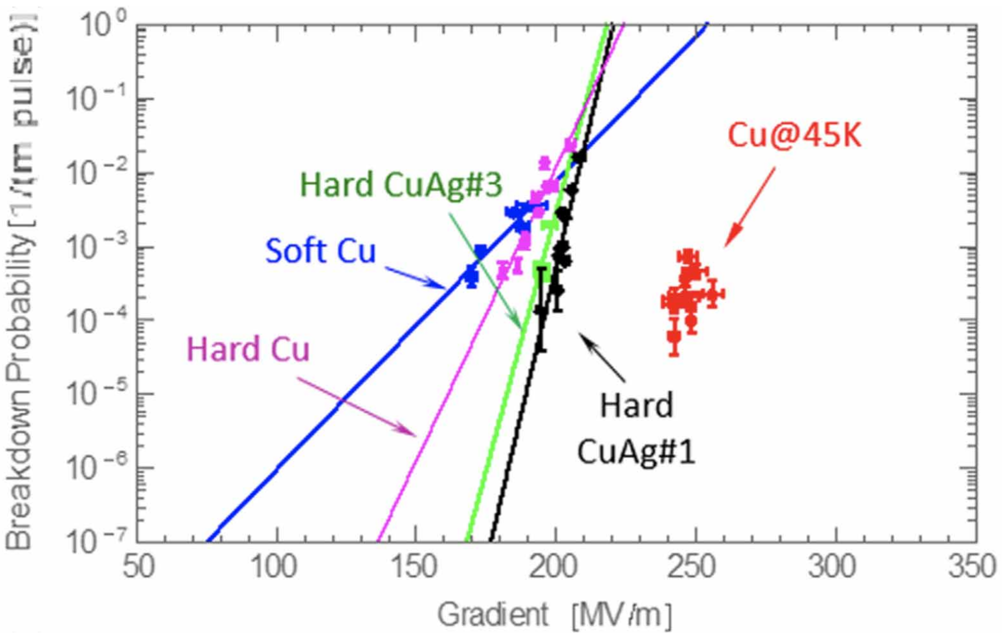

Cahill, A. D., et al. *PRAB* 21.10 (2018): 102002.

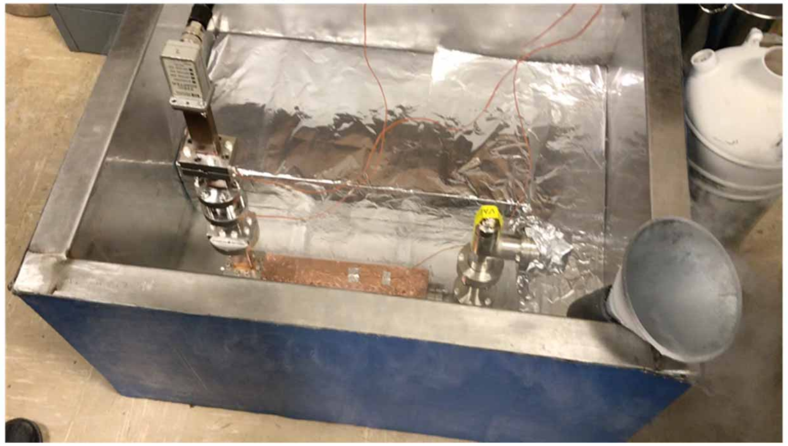

Breakthrough in the Performance of RF Accelerators

RF power coupled to each cell – no on-axis coupling

Full system design requires modern virtual prototyping

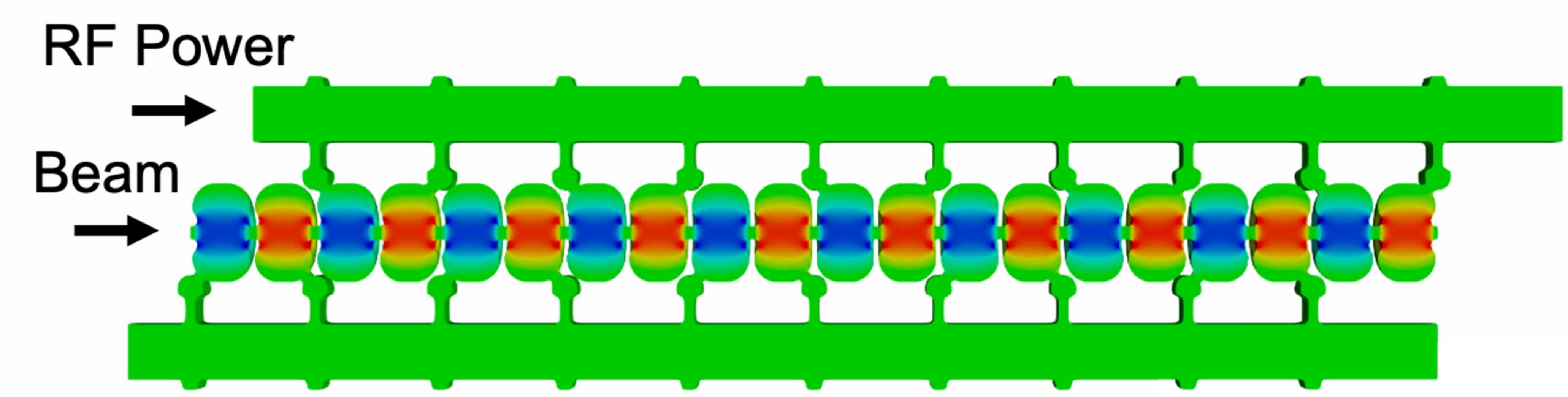

Electric field magnitude produced when RF manifold feeds alternating cells equally

Optimization of cell for efficiency (shunt impedance) $R_s = G^2/P$ [MΩ/m]

- Control peak surface electric and magnetic fields

Key to high gradient operation

Tantawi, Sami, et al. *PRAB* 23.9 (2020): 092001.

Cool Copper Collider as a Higgs Factory

C^3 is based on cryogenic operation and distributed rf coupling

- Dramatically improving efficiency and breakdown rate

Robust operations at high gradient: 120 MeV/m

Target 250/550 GeV center of mass with 70/120 MeV/m in an 8 km footprint

C^3 250/550 GeV 8 km Site to Scale

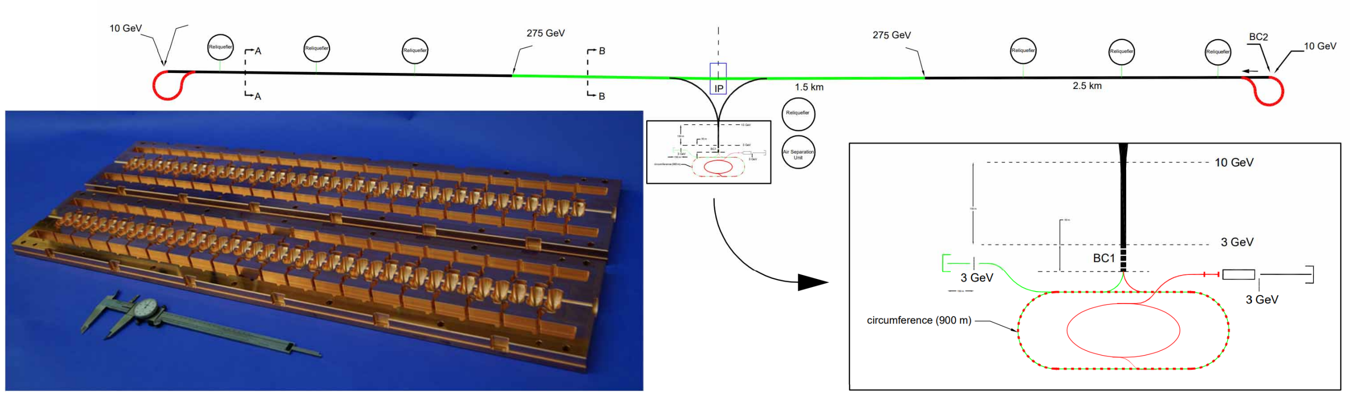

C^3 Prototype One Meter Structure

High Gradient Operation at 150 MV/m

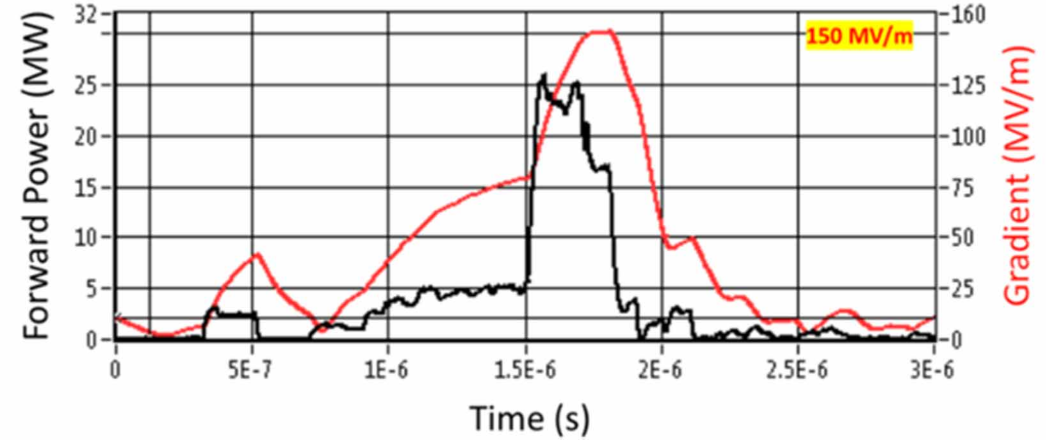

Cryogenic Operation at X-band

Improvement in Breakdown Rate

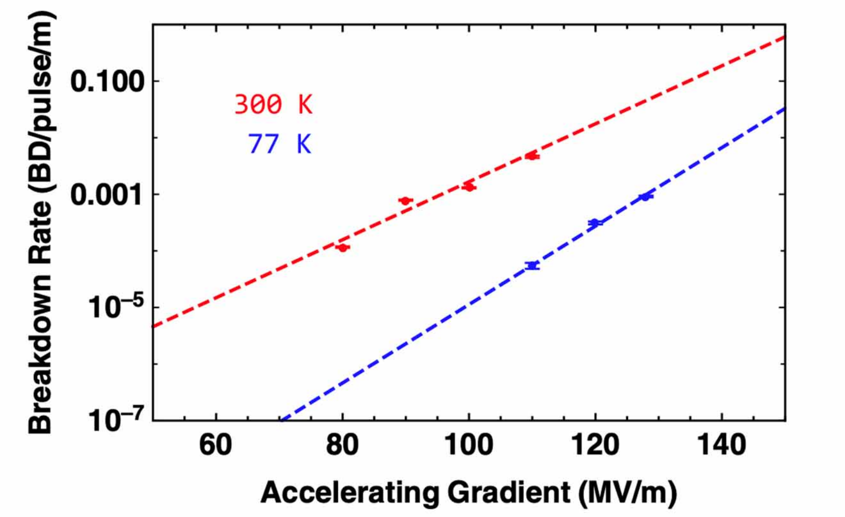

PHYS. REV. ACCEL. BEAMS 24, 093201 (2021)

Ongoing Prototype Structure Development

Incorporate the two key technical advances: Distributed Coupling and Cryo-Copper RF

Main linac utilizes meter-scale accelerating structures, technology demonstration underway

Implement optimized rf cavity designs to control peak surface fields

RF structure optimization to reduce peak E and H-field

RF Structure Optimization

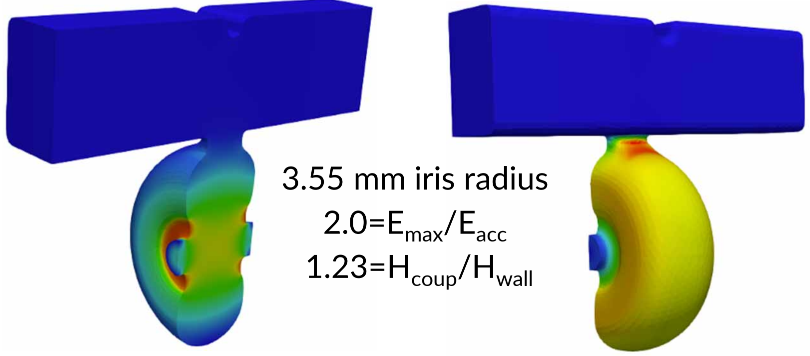

Electric Field

Magnetic Field

M. Shumail, Z. Li

Scaling fabrication techniques in length and including controlled gap

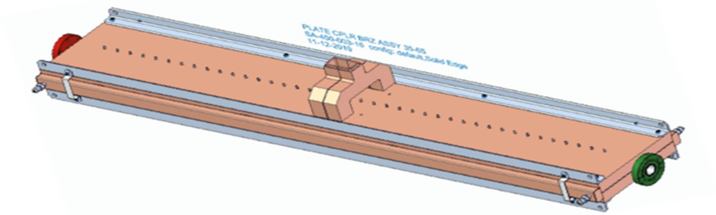

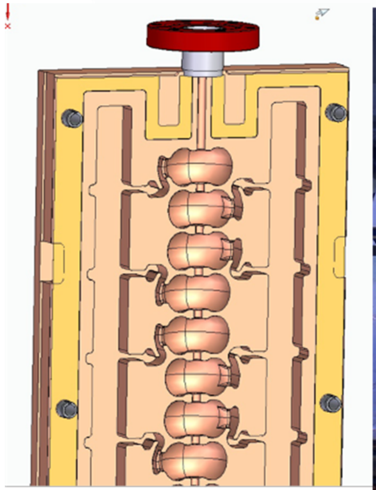

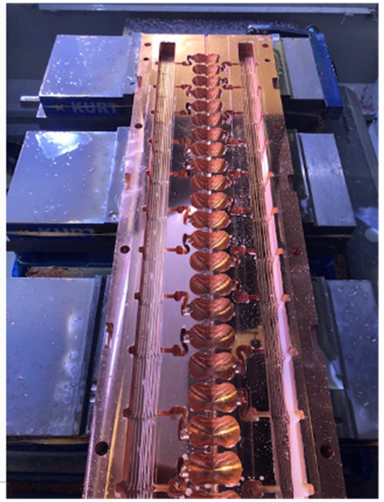

High gradient testing and cryogenic operation

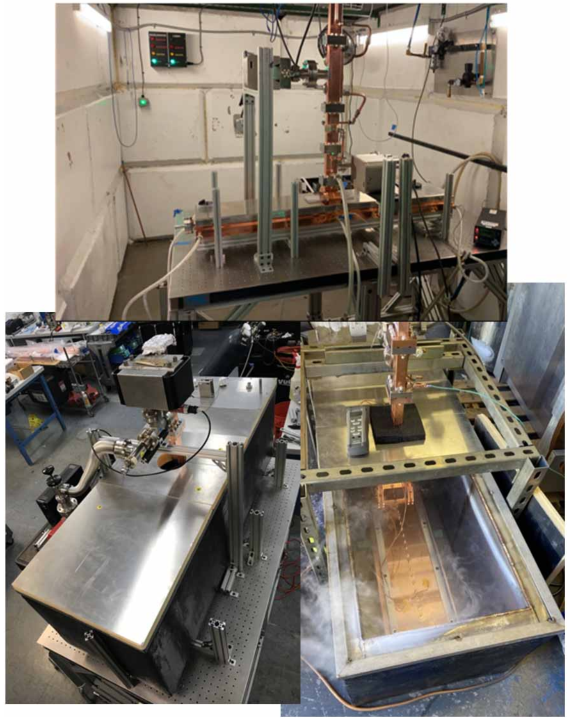

Alignment and Vibrations

System level optimization essential for achieving performance

Beam Dynamics

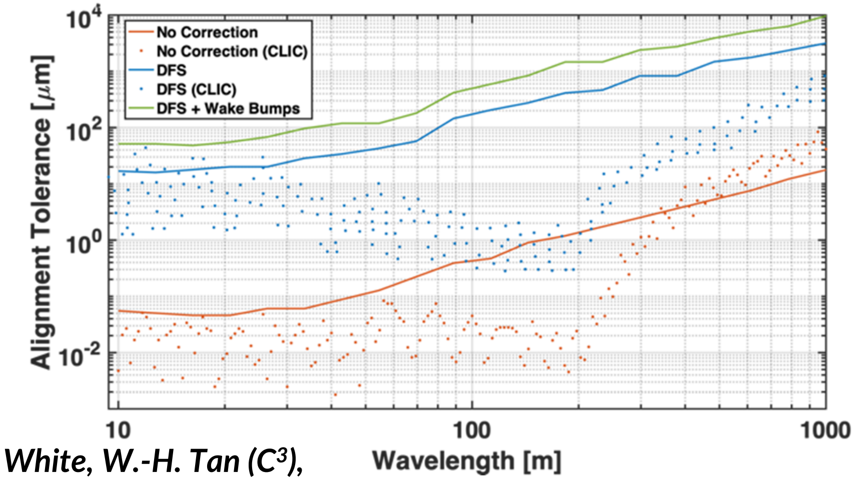

White, W.-H. Tan (C³), Schulte (CLIC)

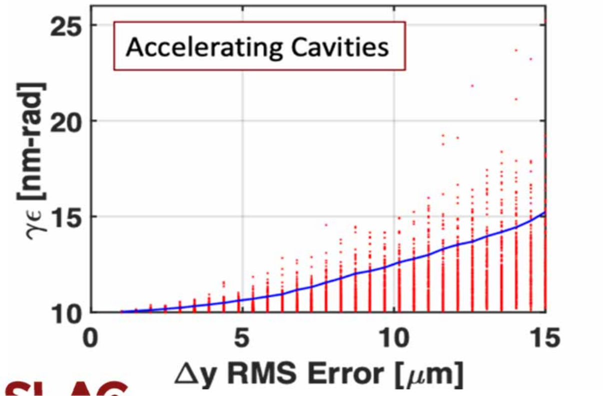

Thermals and Vibration Analysis

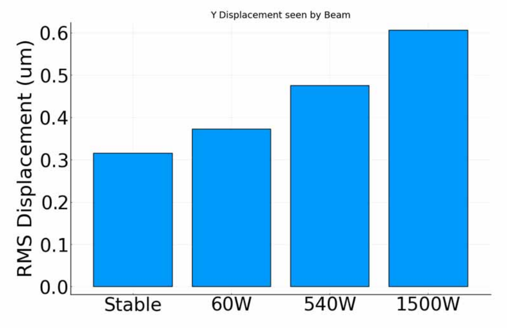

Z. George, V. Borzenets, A. Dhar, D. Palmer

Alignment Parameters	Units	Value
Raft Components	µm	5
Short Range (~10m)	µm	30
Long Range (>200m)	µm	1000
Structure Vert. Vibration	µm	9
Quad Vert. Vibration	nm	15
BPM Resolution	µm	0.1
BPM-Quad Alignment	µm	2

Two-Phase Fluid Simulations

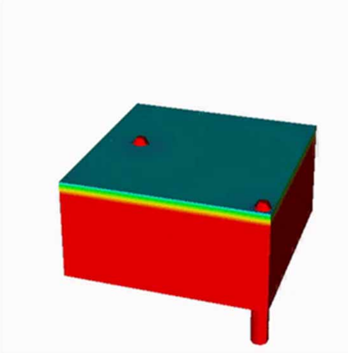

FAMU-FSU College of Engineering

K. Shoele

Precision Short and Long Range Alignment

H. Van Der Graaf

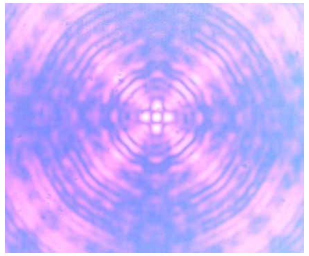

Nikhef

100 nm resolution

Approved effort to test cold

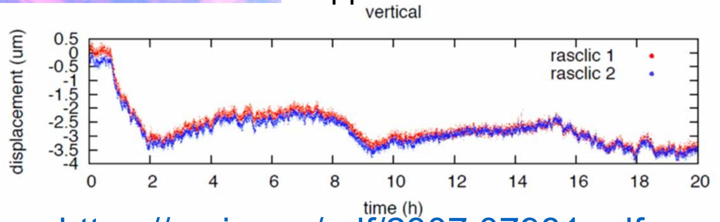

https://arxiv.org/pdf/2307.07981.pdf

Cryomodule Design and Alignment

Up to 1 GeV of acceleration per 9 m cryomodule

Main linac with 5 micron structure alignment

- Combination of mechanical and beam based alignment

Pre-alignment warm, cold alignment by wire, followed by beam based

- Mechanical motor runs warm or cold – no motion during power failure
- Piezo for active alignment

Investigating support and assembly design

Preliminary Alignment and Positioning

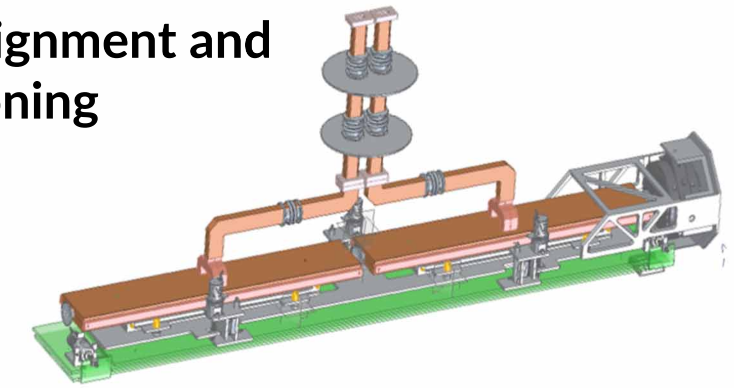

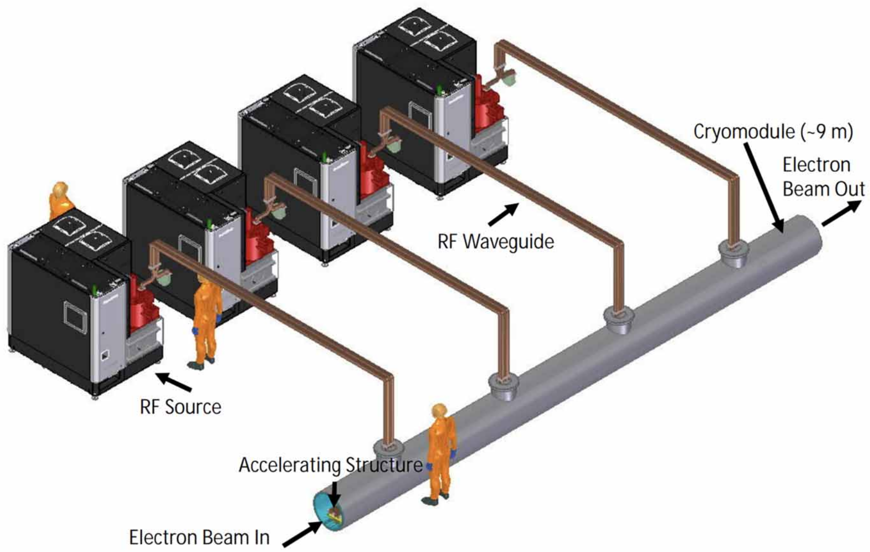

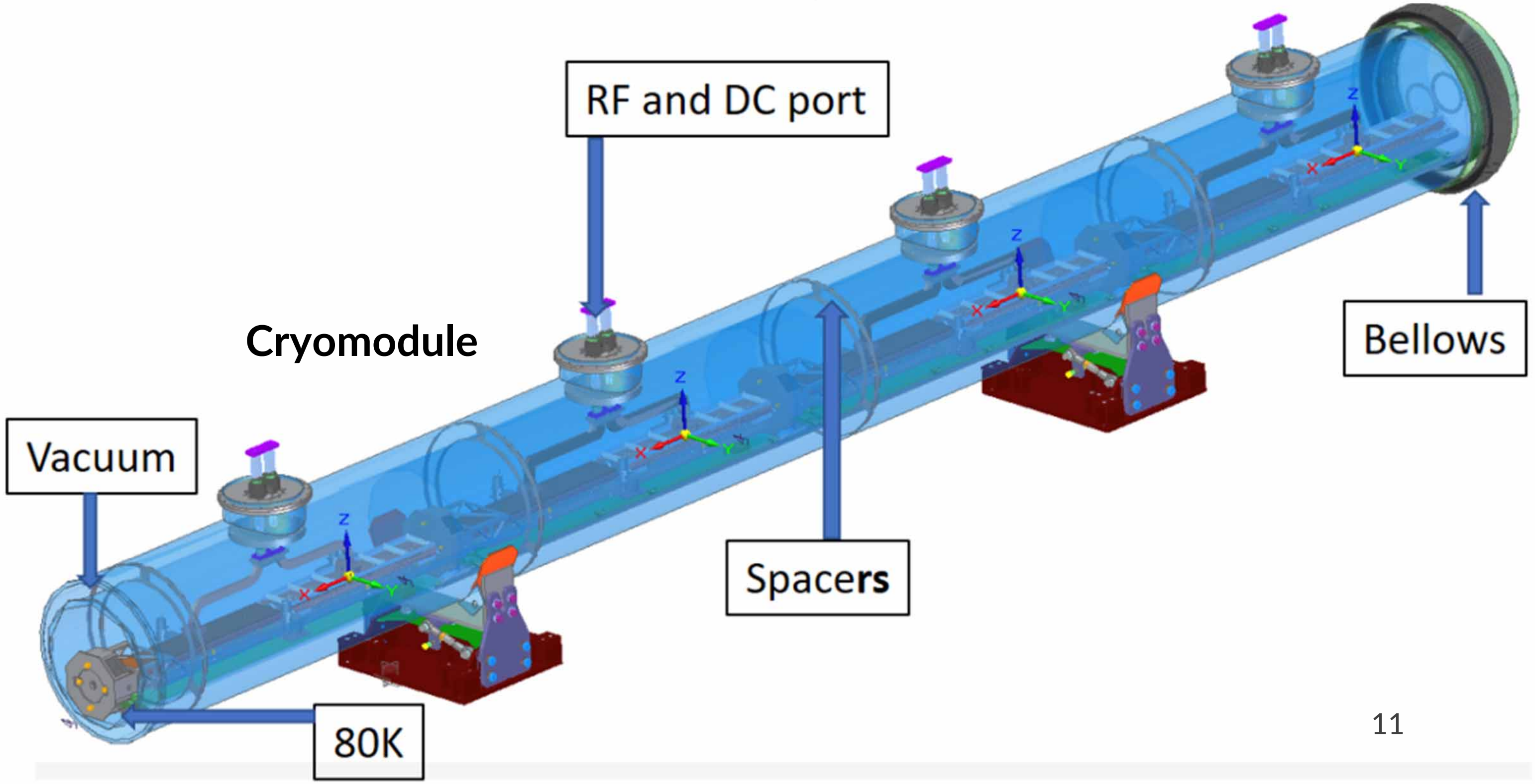

Distributed Coupling Structures Provide Natural Path to Implement Detuning and Damping of Higher Order Modes

Individual cell feeds necessitate adoption of split-block assembly
Perturbation due to joint does not couple to accelerating mode
Exploring gaps in quadrature to damp higher order mode

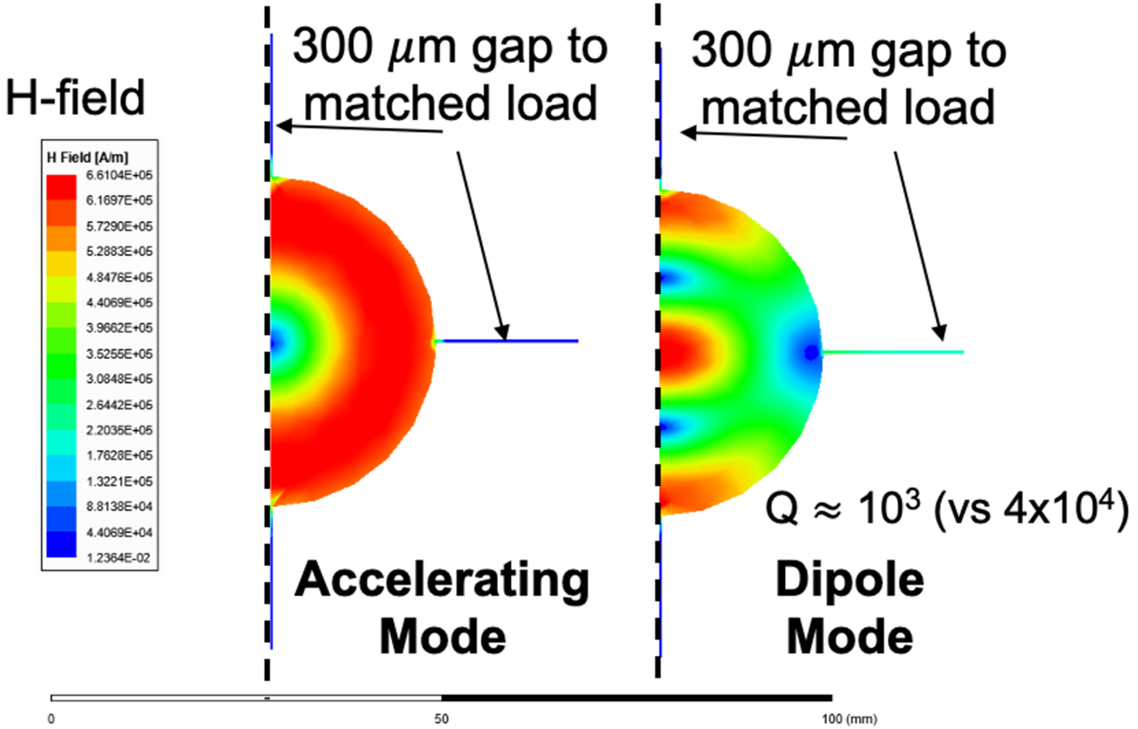

Detuned Cavity Designs

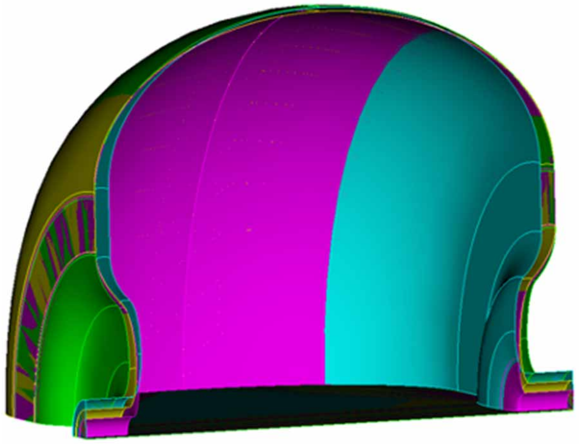

Quadrant Structure

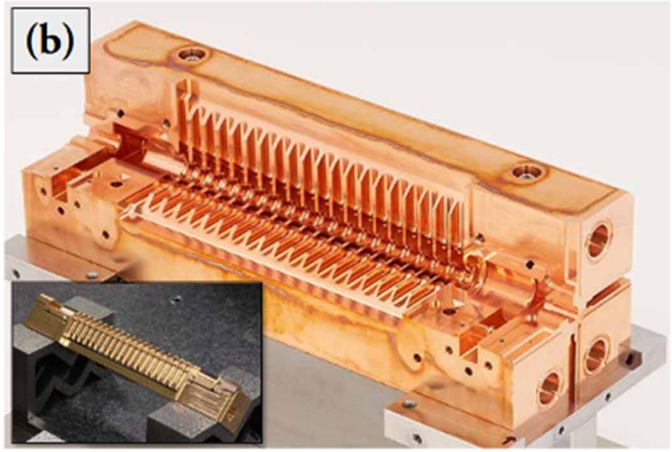

Abe et al., PASJ, 2017, WEP039

Implementation of Slot Damping

Need to extend to 40 GHz / Optimize coupling / Modes below 10^4 V/pC/mm/m

NiCr coated damping slots in development

Kick Factor * Q

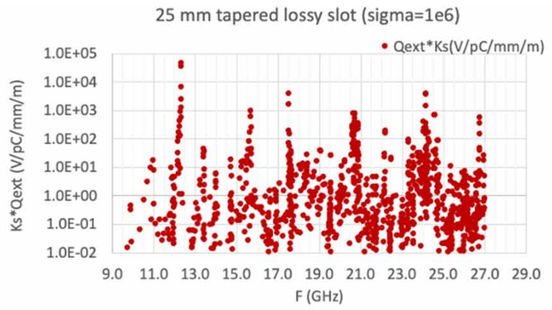

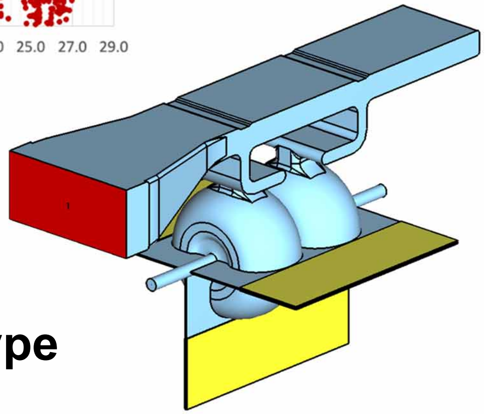

Two Cell Prototype

H. Xu, LANL

Vacuum Space Model

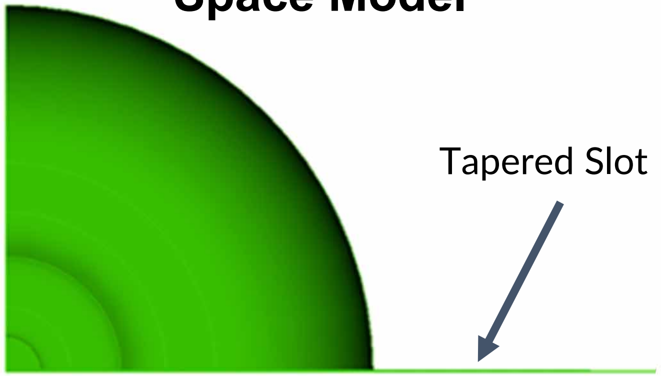

Kick Factor

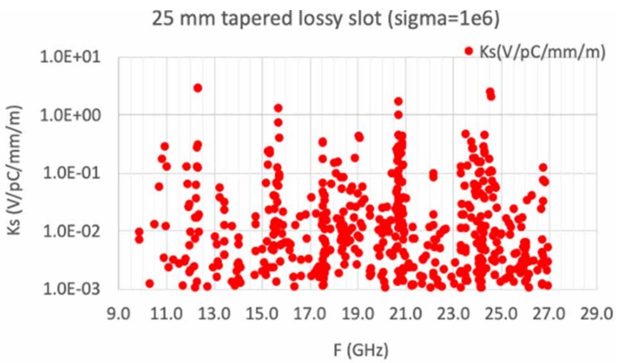

NiCr Tested at 80K

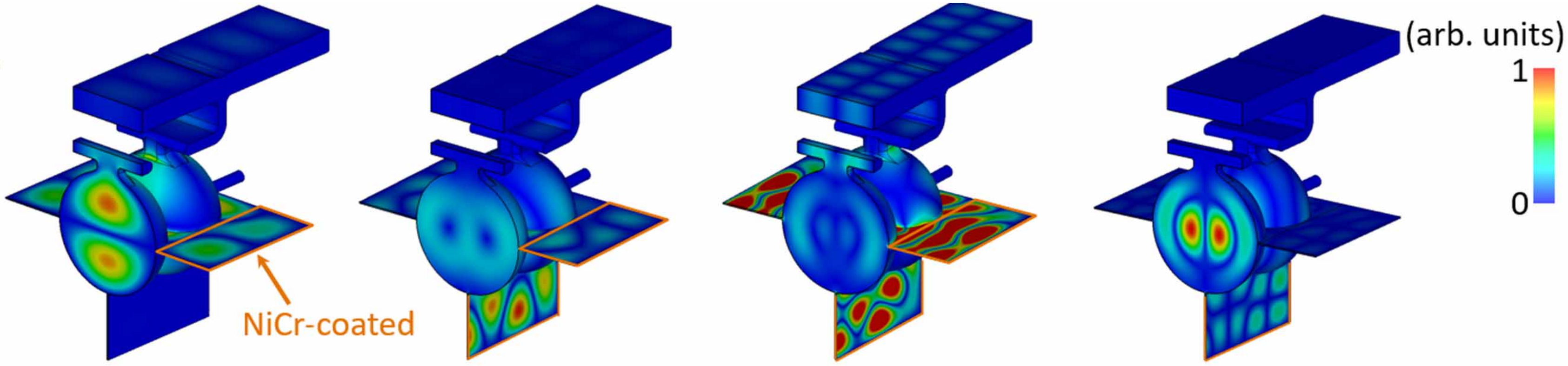

TM110 (9.27 GHz) TM211 (12.28 GHz) TM120 (15.67 GHz) TM121 (17.65 GHz)

Further Cavity Optimization Possible

- Single side coupling iris induces dipole and quad fields
- Coupling hole symmetrization and racetrack shape incorporated to minimize dipole and quad fields

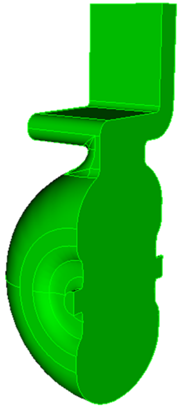

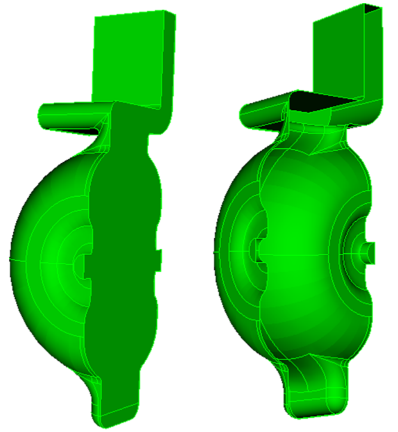

V1-simple-stub
(not ideal cancellation)

V2-symm-stub
(good cancellation)

dipole, quad calculated at 50MV/m

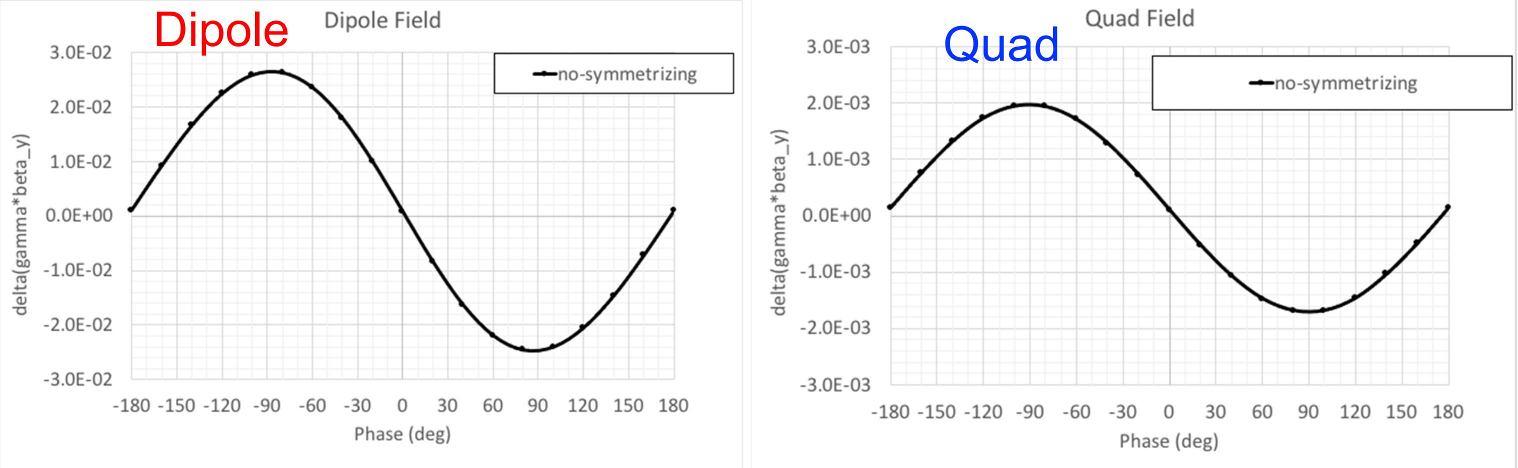

w/o symmetrization

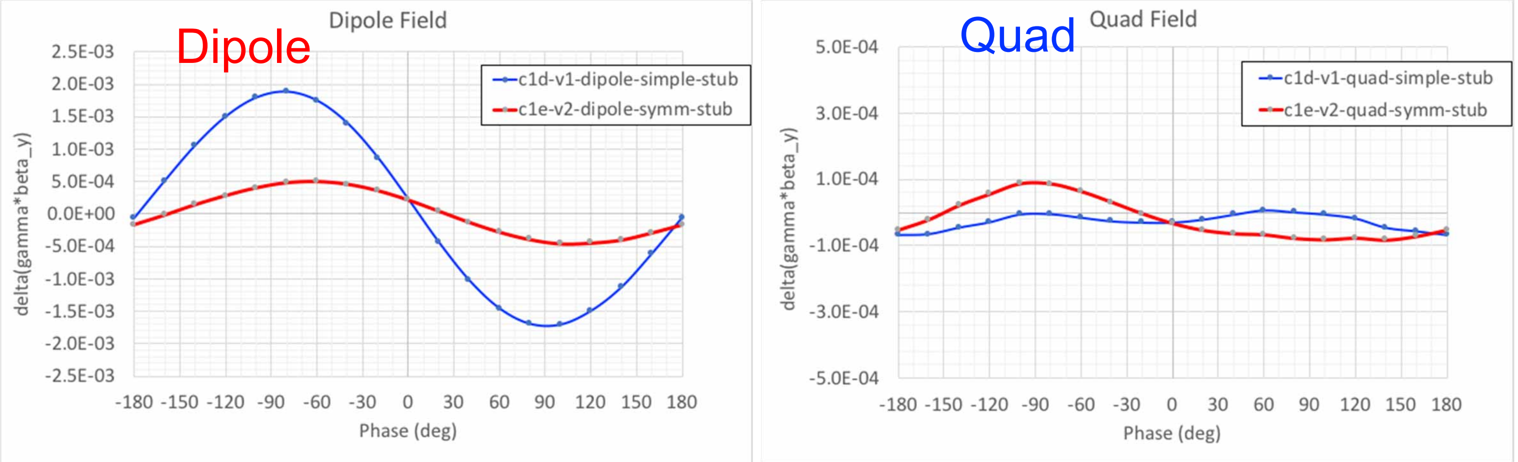

with symmetrization 100X reduction

Zenghai Li

The Complete C^3 Demonstrator

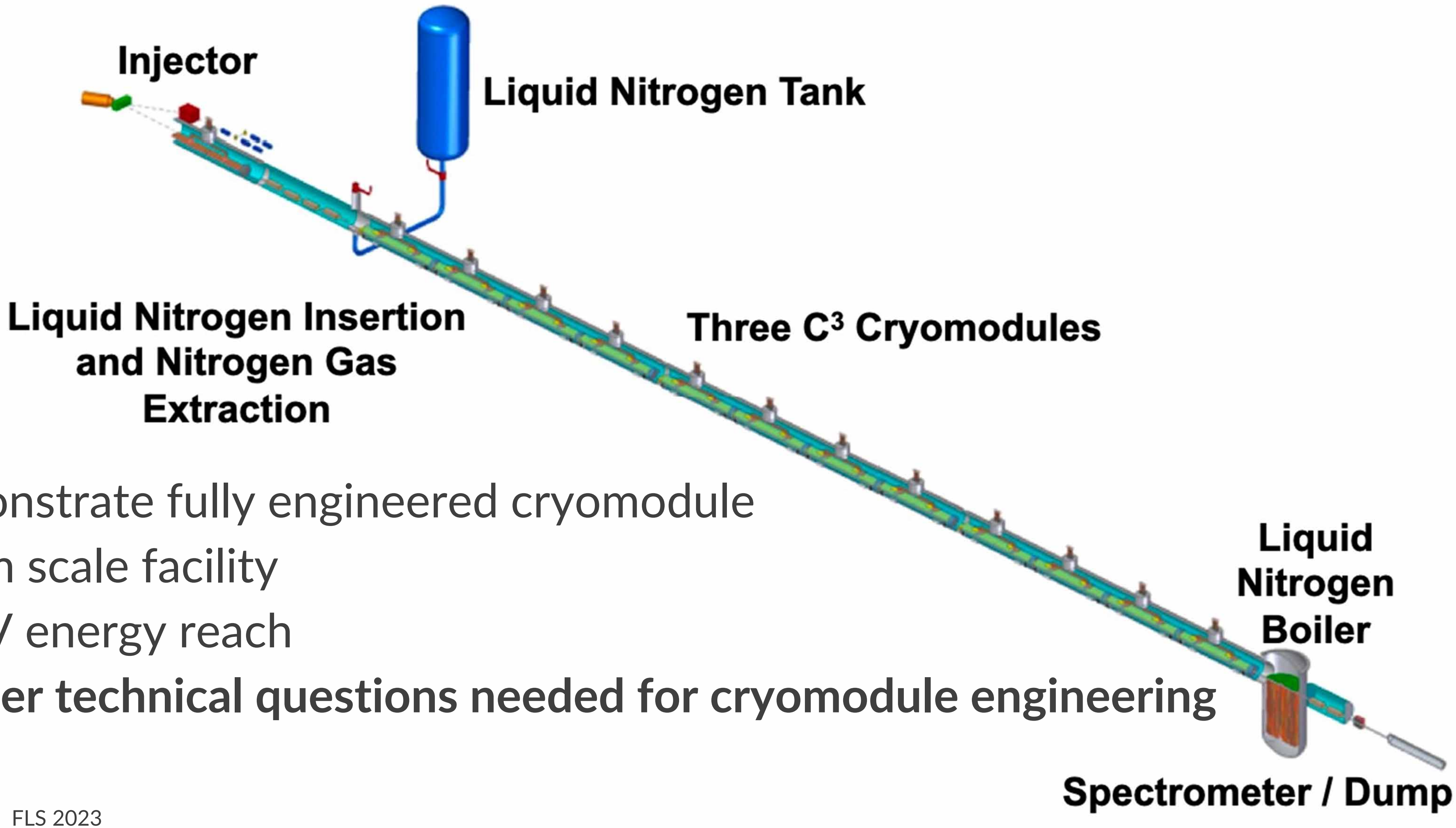

Demonstrate fully engineered cryomodule

~50 m scale facility

3 GeV energy reach

Answer technical questions needed for cryomodule engineering

Outlook for Future Light Sources

Near-Term Use of C^3 Cryomodules

- Provided X-ray flux† depends strongly on the beam energy even for a fully bunched beam
- 1 keV photons, 100 A, 10 fs

	Optical Undulator		Short Period / RF Undulator		Static Undulator
Beam Energy (MeV)	10	32	390	460	1100
Undulator Period	1 micron	10 micron	1.5 mm	2 mm	1.2 cm
photons/shot	4.5E+07	2.9E+08	1.8E+10	2.4E+10	1.0E+11
PSAT (MW)	0.3	2.3	149.3	191.1	843.5

Screening

Seeding

†M. Xie, Nucl. Inst. Meth. A, 445, 59 (2000)

High Repetition Rate Operation

- Reduced thermal load at high gradient with cryogenic operation
- Depends strongly on desired gradient and length of flat top
- Assuming 10 micron alignment -> ~15 kW/m thermal load

Example: C-band, No RF Pulse Compression, 140 MW/m, 150 MeV/m, 50 ns Flat Top, 480 Hz, 15 kW/m

RF Pulse Energy

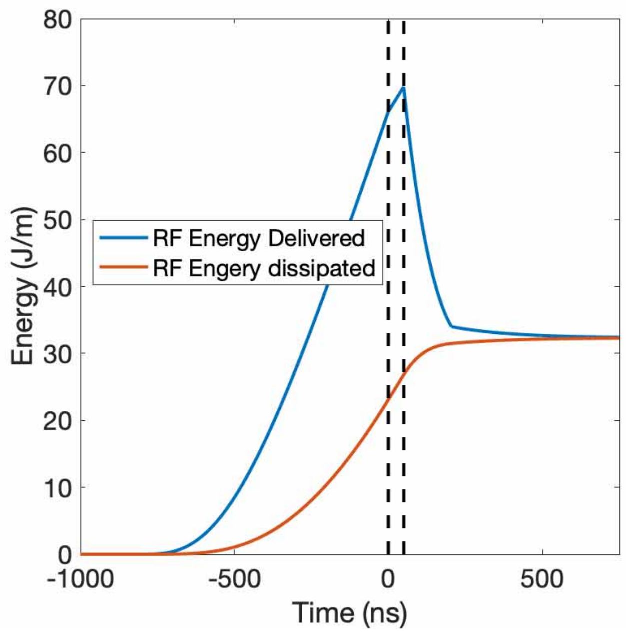

Gradient

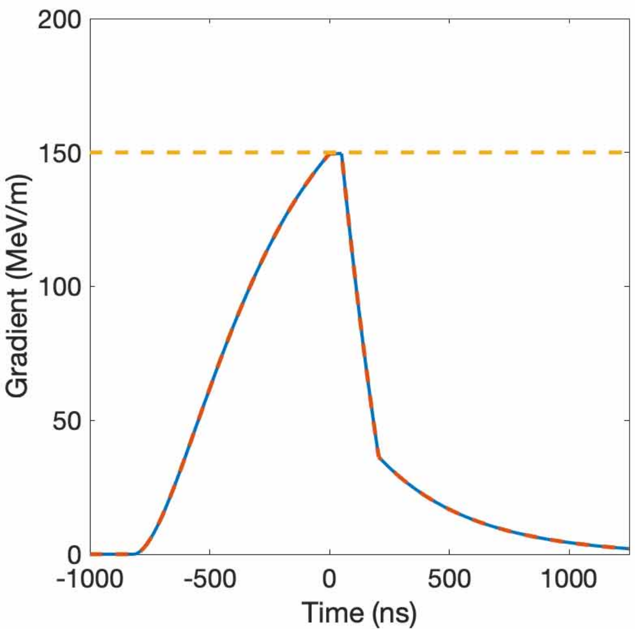

<u>Lowest Frequency for Specified Rep. Rate</u>

10 kHz Operation – 50 MeV/m – X-band
1 kHz Operation – 100 MeV/m – X-band
1 kHz Operation – 70 MeV/m – C-band
360 Hz Operation – 120 MeV/m – C-band
120 Hz Operation – 150 MeV/m – S-band

Compact FEL Performance

- **With 10-100 fs timing resolution**!

Average Brightness

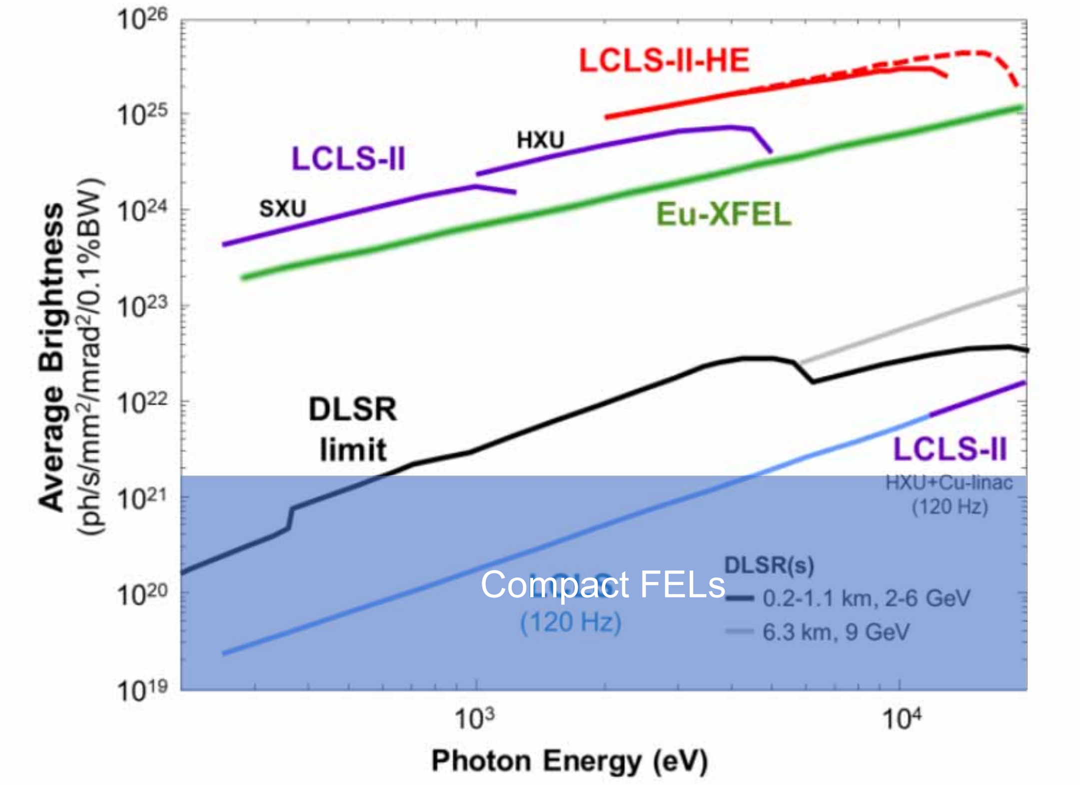

Figure 8: Expected average brightness from LCLS-II and LCLS-II-HE.

T. Raubenheimer, 2018: THE LCLS-II-HE, A HIGH ENERGY UPGRADE OF THE LCLS-II

Peak Brightness

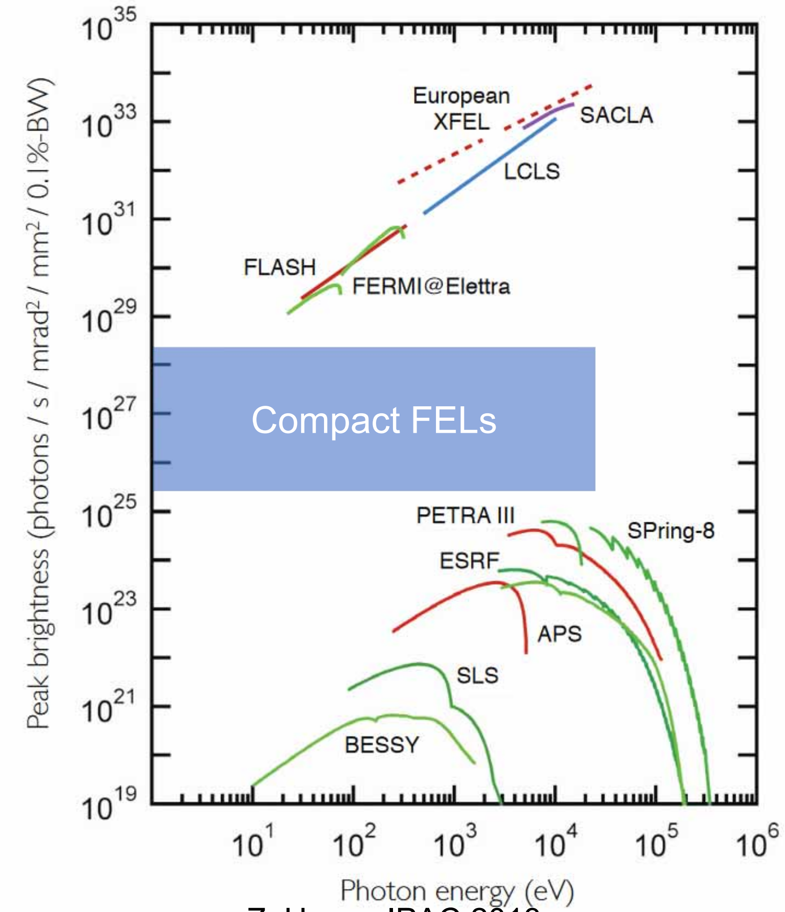

Z. Huang IPAC 2013

UCLA C-band Cryogenic Photoinjector Project

UCLA

- **Cryogenic C-band photoinjector at extreme high brightness for FEL**

Profit from very high fields (up to 250 MV/m) on photocathode;
higher spatial harmonics

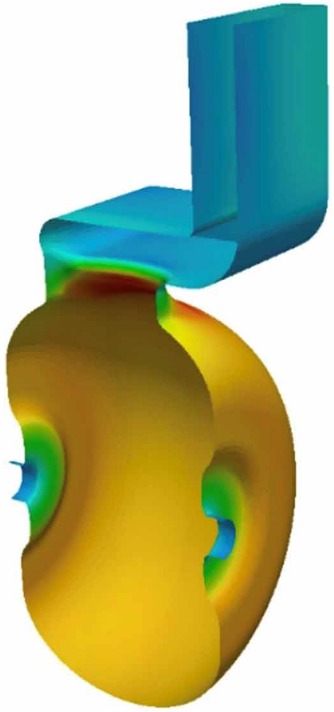

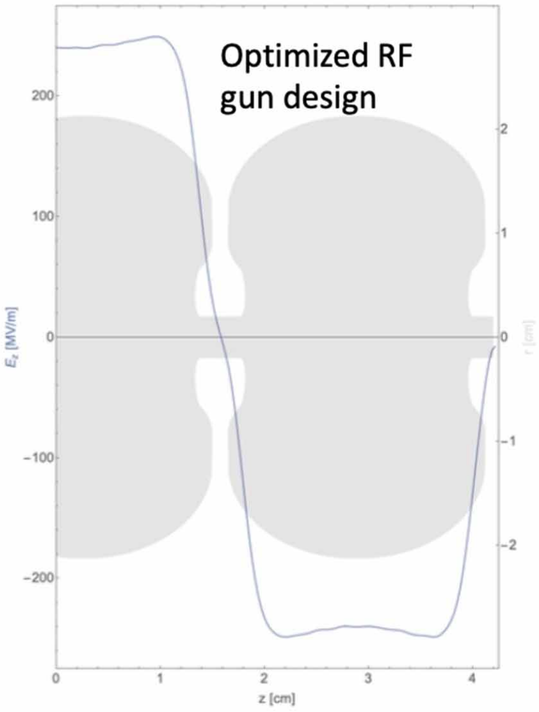

$\boldsymbol{E_0}$=250 MV/m

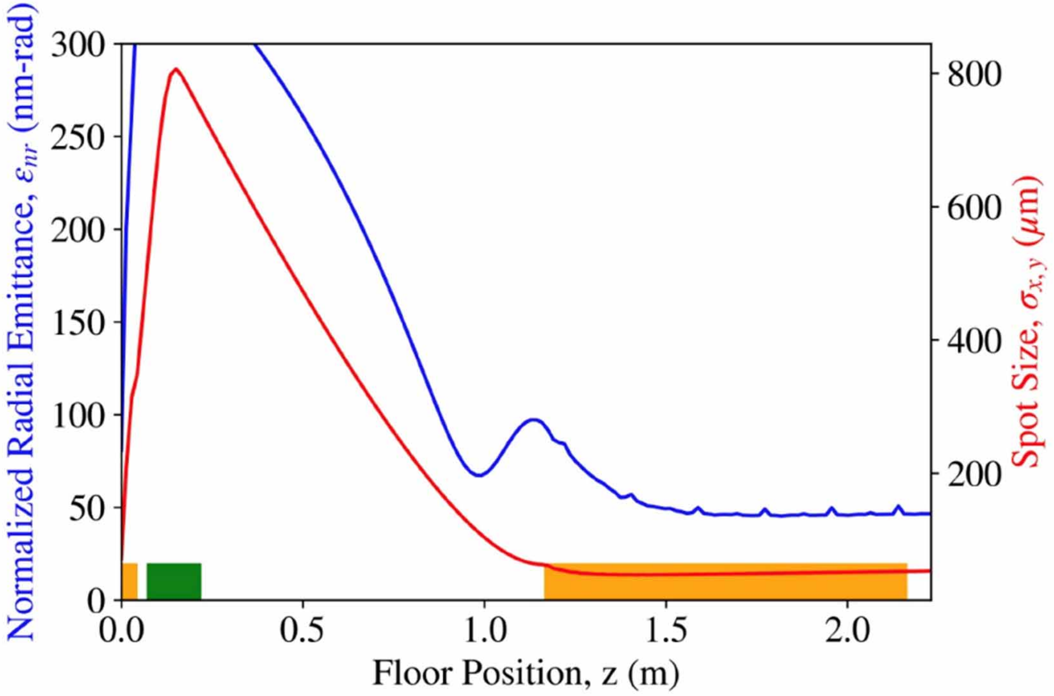

R. Robles, et al., Phys. Rev. Accel. Beams 24, 063401 (2020)

Questions?